

975 nm 量子阱激光二极管的质子位移损伤

刘翠翠¹, 井红旗², 林楠^{2,3}, 郭刚^{1*}, 马骁宇^{2,3**}¹中国原子能科学研究院国家原子能机构抗辐照应用技术创新中心, 北京 102413;²中国科学院半导体研究所光电子器件国家工程中心, 北京 100083;³中国科学院大学材料科学与光电技术学院, 北京 100049

摘要 针对典型卫星轨道辐射环境下激光二极管(LD)的可靠性评估问题,对自研的975 nm GaAs基量子阱(QW)LD开展了10 MeV质子、 $3 \times 10^8 \sim 3 \times 10^{11} \text{ cm}^{-2}$ 注量的地面模拟辐照实验。结合蒙特卡罗软件仿真模拟和数学分析方法,全面研究了器件位移损伤退化规律,以及不同注量、不同辐照缺陷对器件功率特性、电压特性和波长特性等关键参数的影响。结果显示,质子辐照会引入非辐射复合中心等缺陷并破坏界面结构,导致载流子浓度降低、光电限制能力下降,宏观上体现为器件阈值电流增加、输出功率下降、波长红移和单色性受损。同时, $3 \times 10^{10} \text{ cm}^{-2}$ 以上注量的10 MeV质子等效位移损伤剂量辐照会对975 nm QW LD性能产生较大影响。

关键词 量子光学; 量子阱激光二极管; 质子; 位移损伤效应; 性能评估

中图分类号 TN248.4 **文献标志码** A

DOI: 10.3788/AOS222064

1 引言

光的应用让已知的世界更加便捷,也让未知的世界更加广阔。在更先进的光学动力系统帮助下,人类未来的脚步也将踏向更遥远的深空。对于GaAs基半导体激光二极管(LD),尤其是量子阱(QW)LD,电子被限制在一个有限的区域内,电子的状态波函数所对应的波矢一定,即形成量子化的二维电子气,可发射高质量近红外相干激光。由于此波段激光指向性好、能量集中和传输距离远,故其成为了空间、核应用等领域中远距离无线能量传输的首选^[1-2]。然而,太阳质子事件、Van Allen辐射带和银河宇宙射线会导致空间中存在大量质子、电子、重离子等高能粒子^[3-4],核环境下也存在大量中子等高能粒子,这些粒子会诱发半导体LD的位移损伤等辐射效应^[5-6],甚至对LD产生致命威胁。

早在1967年GaAs基LD诞生之初,Compton等^[7]便开展了LD辐射效应研究,并在电子辐照后观察到了阈值电流增大的现象。20世纪80年代QW LD诞生后不久因其优异性能迅速被广泛研究,也逐渐揭示了其敏感参数的辐射退化规律和基本机制。Evans等^[8]开展了能量为5.5 MeV和200 MeV的质子辐照实验,发现器件辐射损伤的主要影响是体复合增加导致内损耗增加。Boutillier等^[9]对852 nm GaInAsP单量子阱LD开展了31 MeV质子、 $5 \times 10^{12} \text{ cm}^{-2}$ 注量的辐照实

验,发现器件光电特性的退化与辐照引入杂质所导致的非辐射载流子寿命下降密切相关。国内激光器研究虽然发展得较晚,但是西北核技术研究所、中国人民解放军空军工程大学、中国科学院长春光学精密机械与物理研究所和中国科学院新疆理化技术研究所等对其辐射效应问题也开展了诸多实验研究^[10-13]。

为探究975 nm GaAs基QW LD在辐射环境下的位移损伤退化规律和机理,国内外均开展了不同条件下的辐照实验研究和理论分析,但实验方法主要集中在电子、中子、伽马射线和高能质子,对于10 MeV中能质子辐照和考核评估技术的研究内容较少。随着新应用场景的开拓,新型高性能器件的发展日新月异,针对今后空间通信、传能等国产化应用技术布局,QW LD位移损伤效应考核的实验方法需实时跟进。为了继续明确器件的最劣辐照偏置条件、辐照剂量(注量)、剂量率(注量率)、能量、粒子种类和失效判据等,开展了自研高性能975 nm GaAs基QW LD质子辐照位移损伤效应退化规律和效应机理研究。

2 QW LD位移损伤模拟

2.1 器件结构及工作机理

本实验所用的975 nm高功率QW LD器件样品是中国科学院半导体研究所研制的,采用金属氧化物化学气相沉积(MOCVD)设备制备。使用的生长源为

收稿日期: 2022-11-28; 修回日期: 2022-12-26; 录用日期: 2023-02-10; 网络首发日期: 2023-03-09

基金项目: 国家重点研发计划(2018YFB117300)、中核集团“青年英才”科研项目(11FY212306000801)

通信作者: *ggg@ciae.ac.cn; **maxy@semi.ac.cn

Ⅲ族金属有机化合物,即三甲基铟(TMIn)、三甲基镓(TMGa)、三甲基铝(TMAl)。砷烷(AsH_3)为V族源,硅烷(SiH_4)、四氯化碳(CCl_4)为掺杂剂。样品基本结构如表1所列,外延结构从下至上的组成为500 μm n-掺杂GaAs衬底层(Substrate)、160 nm Al组分渐变的N-AlGaAs过渡层(N-transition)、950 nm N- $\text{Al}_{0.291}\text{GaAs}$ 限制层(N-cladding)、480 nm N- $\text{Al}_{0.295}\text{GaAs}$ 渐变层(N-gradient)、480 nm N- $\text{Al}_{0.240}\text{GaAs}$ 波导层(N-waveguide)、40 nm Al组分渐变的无掺杂AlGaAs势垒层(Barrier)、7.9 nm 无掺杂 $\text{In}_{0.160}\text{Ga}_{0.840}\text{As}$ QW(QW)、40 nm Al组分渐变的无掺杂AlGaAs势垒层(Barrier)、1000 nm P- $\text{Al}_{0.355}\text{GaAs}$ 波导层(P-waveguide)和150 nm 高掺杂P-GaAs帽层(Cap),带隙结构如图1所示,其中 E_g 为带隙宽度, n 为折射率。LD的发光区条宽为100 μm ,中心波长为975 nm,输出功率大于10.5 W或12 A。随着正向偏置的增加, $\text{In}_{0.160}\text{Ga}_{0.840}\text{As}$ QW区形成电子势阱和空穴势阱俘获N区注入的电子和P区注入的空穴,逐渐使受激辐射强于受激吸收。同时,器件

两端的解理面构成谐振腔连同内部增益介质实现激光光子的振荡和增生。在光子增益大于损耗之后,在前腔面处出射特定波长的激光。

表1 QW LD的结构参数
Table 1 Structural parameters of QW LD

Epitaxial layer	Material	Thickness / nm
Cap layer	$\text{P}^+\text{-GaAs}$	150
P-cladding layer	$\text{P-Al}_{0.355}\text{GaAs}$	1000
Barrier	$\text{Al}_{0.154}\text{GaAs}$ to $\text{Al}_{0.240}\text{GaAs}$	40
Single QW	$\text{In}_{0.160}\text{GaAs}$	7.9
Barrier	$\text{Al}_{0.240}\text{GaAs}$ to $\text{Al}_{0.154}\text{GaAs}$	40
Waveguide layer	$\text{Al}_{0.240}\text{GaAs}$	480
N-gradient layer	$\text{N-Al}_{0.295}\text{GaAs}$	480
N-cladding layer	$\text{N-Al}_{0.291}\text{GaAs}$	950
N-transition layer	N-GaAs to $\text{N-Al}_{0.285}\text{GaAs}$	160
Substrate	GaAs buffer	500

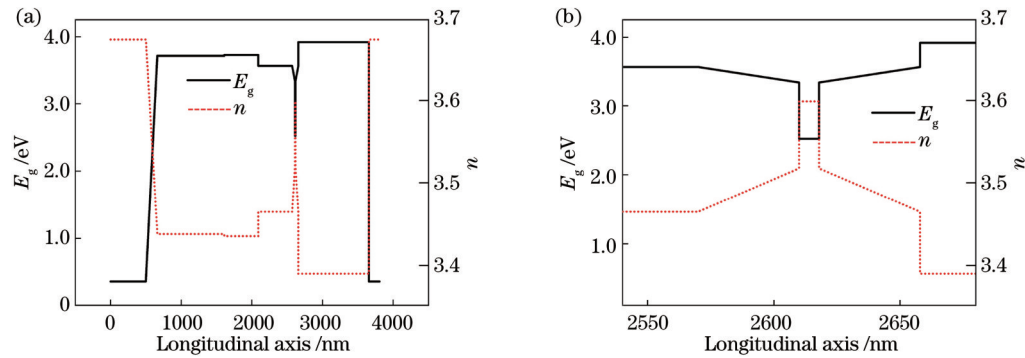


图1 LD的带隙结构和折射率分布。(a)器件整体;(b) QW局部

Fig. 1 Band gap structure and refractive index distribution of LD. (a) Whole device; (b) QW local

2.2 器件位移损伤模拟

将QW LD结构简化为150 nm GaAs、1040 nm AlGaAs、7.9 nm GaInAs、2590 nm AlGaAs等外延层,以及500 nm GaAs衬底所组成的结构,并基于TRIM软件利用蒙特卡罗方法获取了10 MeV质子入射器件后的分布,如图2(a)所示。可以发现,10 MeV质子在该结构中的穿透深度约为418 μm ,已完全贯穿至器件衬底区域,因此大部分能量会沉积在器件AlN散热陶瓷中。图2(b)为欧姆接触层至衬底层中由10 MeV质子引入的各类空位缺陷分布。图2(c)为空位缺陷整体分布。可以发现,在各界面处,尤其是InGaAs/AlGaAs阱垒界面处会出现一个缺陷密度峰值,说明辐照后波导层与限制层界面、限制层与阱垒界面处均产生了较高浓度的 V_{Ga} 、 V_{As} 、 V_{Al} 等空位缺陷^[3,14]。由图2(b)所示可知,QW区总的峰值空位率约为 $1.2 \times 10^{-4} \text{ A}^{-1} \cdot \text{proton}^{-1}$,说明10 MeV质子累积辐照注量为 $3 \times 10^{11} \text{ cm}^{-2}$ 时可产生的缺陷数量约为 $3.6 \times 10^{15} \text{ cm}^{-2}$,虽然这个数量相比于靶原子数量不高,但这些缺陷对

界面的破坏会削弱QW的光电限制作用,光子和电子向有源区以外泄漏会导致器件输出光功率下降,而辐照缺陷增强了非辐射复合中心的作用,进而引起内量子效率下降^[15]。同时,辐照缺陷也带来了材料层面的损伤,器件工作时在缺陷处会产生热量集中,也会导致器件发光腔面和谐振腔内出现光学灾变损伤(COD)的概率增加。

3 实验及结果分析

3.1 实验方案

在航天工程实践中,常采用10 MeV质子等效位移损伤剂量(DDD)来描述电子器件的位移损伤,结合该方法设计的辐照实验条件如表2所示。该实验在中国原子能科学研究院HI-13串行加速器的重离子单粒子效应实验终端开展。在辐照过程中LD处于室温、无偏压和真空状态,各条件下的辐照时间均为1000 s,并在辐照前后测试分析了器件性能。

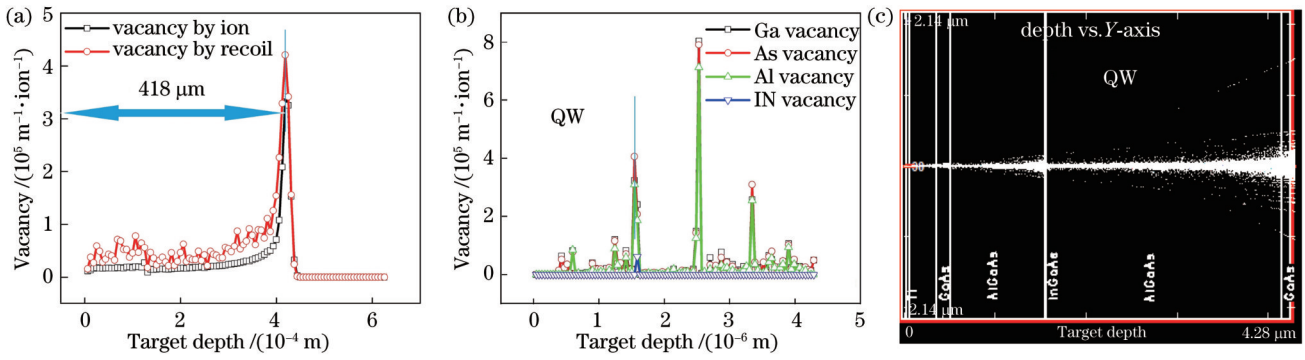


图 2 10 MeV 质子对 LD 的作用。(a) LD 中空位缺陷来源;(b)外延层中空位缺陷的类型;(c)外延层中的空位缺陷分布
Fig. 2 Effect of 10 MeV proton on LD. (a) Source of vacancy defects in LD; (b) types of vacancy defects in epitaxial layers; (c) distribution of vacancy defects in epitaxial layers

表 2 质子辐照实验参数

Table 2 Proton irradiation experimental parameters

Sample	Energy /MeV	Fluence / (cm ⁻²)	DDD / (MeV·g ⁻¹)
LD 1	10	3×10 ⁸	2.37×10 ⁶
LD 2	10	3×10 ⁹	2.37×10 ⁷
LD 3	10	3×10 ¹⁰	2.37×10 ⁸
LD 4	10	1×10 ¹¹	7.91×10 ⁸
LD 5	10	3×10 ¹¹	2.37×10 ⁹

3.2 光学性能分析

图 3 是质子辐照前后 LD 的激光光谱。可以看到, 经质子辐照后 LD 激光峰值强度明显衰退, 且衰退程度与 DDD 的增加正相关, 同样与质子注量也呈明显的

正相关。经计算, 辐照后的激光强度分别衰退至原始数值的 96.8%、93.3%、88.9%、57.8%、56.1%。同时, 质子辐照后器件的光束单色性受损, 杂峰增加且中心波长红移, 但红移程度与注量的线性关系不明显。根据 LD 出光波长与材料禁带宽度的关系, 综合考虑波长红移和杂峰增加的现象, 该结果可能是由辐照产生的深能级陷阱缺陷和界面态导致的^[16]。由于深能级陷阱形成的非辐射复合中心提高了非辐射复合电流占比, 辐照诱生的界面态也会导致 QW 对光场的限制能力下降, 故中心波长两侧杂峰增加。由于入射粒子及其反冲核携带的能量较高, 故辐照缺陷也会导致 QW 混杂现象增强^[17-18], QW 内的元素可能获得能量扩散至势垒或产生核反应而引起浓度降低, 因而产生带隙

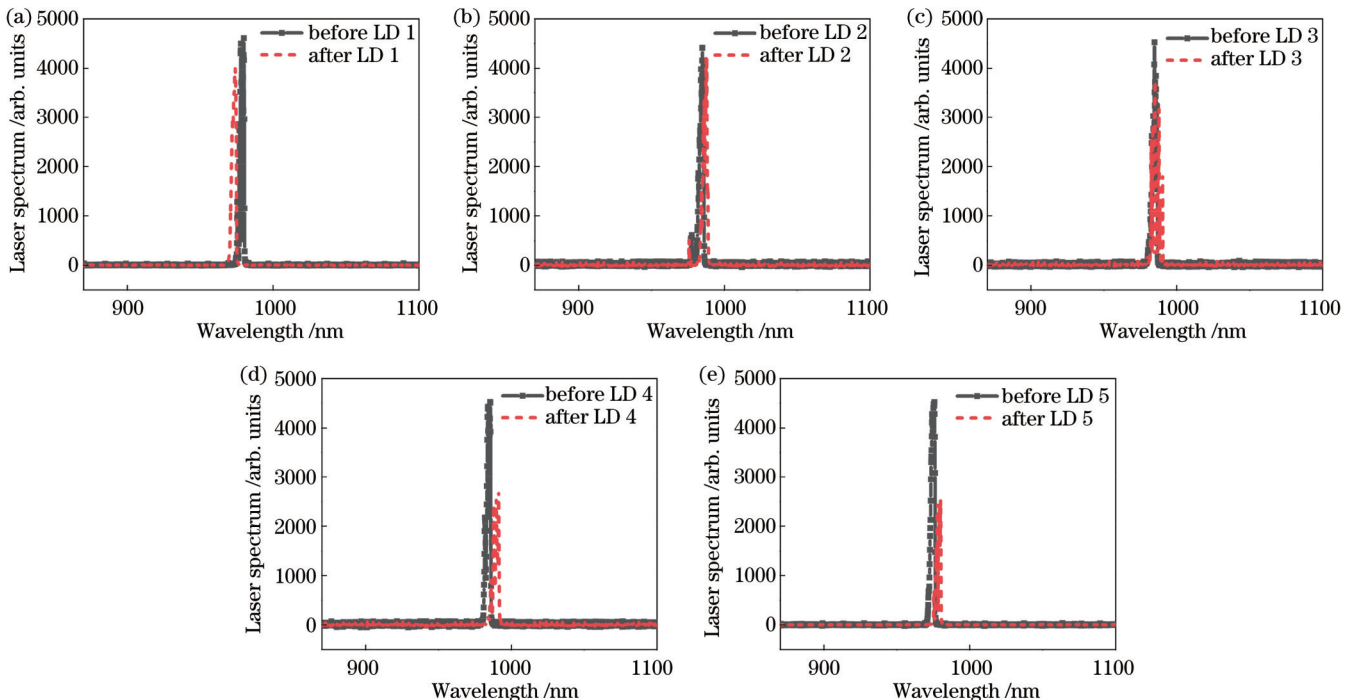


图 3 10 MeV 质子射入 LD 前后的激光光谱。(a) 3×10⁸ cm⁻²; (b) 3×10⁹ cm⁻²; (c) 3×10¹⁰ cm⁻²; (d) 1×10¹¹ cm⁻²; (e) 3×10¹¹ cm⁻²
Fig. 3 Laser spectra of LDs before and after 10 MeV proton injected. (a) 3×10⁸ cm⁻²; (b) 3×10⁹ cm⁻²; (c) 3×10¹⁰ cm⁻²; (d) 1×10¹¹ cm⁻²; (e) 3×10¹¹ cm⁻²

变窄、波长红移的现象。非辐射复合的增加会导致热损耗增加,而半导体带隙宽度随着温度的升高会降低,因此也会导致波长红移现象的出现。

当 LD 的注入电流 I 大于阈值电流 I_{th} 时,即 $I > I_{th}$ 时,LD 的相干辐射强于非相干辐射,半导体激光器的输出光功率 P_{out} 与注入电流 I 近似满足线性关系,故 P_{out} 的值为

$$P_{out} = \eta_D (I - I_{th}), \quad (1)$$

式中: η_D 为外微分量子效率,也称为斜率效率,其值表示注入载流子转化为光子的能力,即描述 LD 相干辐射效率的物理量。对于端面反射率分别为 R_1, R_2 的 QW LD, η_D 可以表示为

$$\eta_D = \frac{\eta_i hc}{\lambda q} \times \frac{\alpha_m}{\alpha_m + \alpha_i} = \frac{\eta_i}{1 + \frac{2\alpha L}{\ln[1/(R_1 R_2)]}}, \quad (2)$$

式中: c 为光速; h 为普朗克常数; λ 为 LD 的中心波长; q 为元电荷电量; α_m 为腔面光损耗; α_i 为内损耗; η_i 为内量子效率,表示注入载流子中进行辐射复合部分的占比,其公式为

$$\eta_i = \frac{1/\tau_R}{1/\tau_R + 1/\tau_{NR}}, \quad (3)$$

式中: τ_R 为辐射复合载流子寿命; τ_{NR} 为非辐射复合载流子寿命。可见,内量子效率 η_i 直接决定斜率效率大小,故对输出功率的影响也十分显著。由于有源区的杂质、缺陷、界面态和 QW 载流子泄漏等因素的影响,故内量子效率满足 $\eta_i < 1$, 其值主要由载流子注入效率、载流子限制效率和辐射复合效率等因素决定。QW 内部缺陷和界面态增加会导致非辐射复合载流子寿命 τ_{NR} 下降,辐射复合效率下降,非辐射复合占比增加,进而导致内量子效率 η_i 下降,外微分量子效率 η_D 也因内损耗 α_i 的增加而下降,宏观上体现为输出功率 P_{out} 下降。

3.3 功率性能分析

图 4 为采用 10 MeV 质子辐照前后 LD 的 P_{out} - I 特性关系。可以发现:辐照后 LD 1 的阈值电流和 12 A 处的输出功率几乎没变;辐照后 LD 2~5 的阈值电流分别从 0.75、0.72、0.47、0.51 A 升至 0.76、0.98、0.69、0.75 A (上升率分别为 1.33%、36.11%、46.81%、47.06%),在 12 A 处的输出功率分别从 10.72、10.54、10.61、11.13 W 降至 10.29、8.84、8.00、8.37 W (下降率分别为 4.01%、16.13%、24.60%、24.80%)。另外,发现随着注入电流 I 的增加,非辐射复合占比增加,输出功率 P_{out} 逐渐恶化,辐照前后 P_{out} - I 曲线已出现明显区别,表明辐照后的阈值电流出现了一定程度的增加,且增加程度与质子的注量呈现明显的正相关。假设 QW LD 受到质子辐照损伤的程度以损伤因子 n 表示,满足

$$\frac{I_{th}(\varphi)}{I_{th}(0)} = 1 + n\varphi, \quad (4)$$

式中: φ 为质子注量; $I_{th}(\varphi)$ 为经质子辐照后器件的阈值电流; $I_{th}(0)$ 为未辐照器件的阈值电流。将图 4 数据代入式(4)后拟合得到器件的损伤因子 n 的值约为 $1.203 \times 10^{-11} \text{ cm}^2 \cdot \text{proton}^{-1}$ 。由 TRIM 模拟结果可知,在各外延层界面处出现了缺陷率峰值,由这些缺陷形成的界面态会导致 QW 对二维电子气的限制能力降低,形成的缺陷能级会引起受激辐射强度下降,非辐射复合增加。同时,非辐射复合产生的能量转化为热能也会导致器件更易发生 COD 等灾难性损伤。

图 5 为采用 10 MeV 质子辐照前后 LD 的 V - I 特性关系。测试设定电流与实际电流值之间的关系发现辐照前后器件的电流设定关系并未明显改变。将电压电流进行比值即可获得 LD 的串联电阻,且随着驱动电流的增加,载流子浓度和注入电流共同的作用将导致 LD 电流增大、串联电阻减小。质子辐照后器件的电压特性下降现象说明电光转换效率下降是质子辐照引起串联电阻增大导致的^[19]。

3.4 器件能带结构分析

器件外微分量子效率下降的实验现象与 TRIM 模拟的结果相符,说明质子在器件材料内部和异质结界面处引入了缺陷。缺陷的散射作用导致载流子迁移率下降,产生陷阱能级和非辐射复合中心,缺陷俘获电荷会导致异质结界面处电荷积聚。注入粒子与缺陷的诱导作用也会在界面处引发 QW 混杂现象形成渐变结构,从而产生如图 6 所示的折射率由跃变变为缓变和能带弯曲的现象,并导致空间电荷区载流子浓度与载流子寿命 τ 下降、空间电荷区复合电流与扩散电流均下降,以及激光的单色性受损。随着质子注量的增加,器件偏压特性下降程度增加,说明大注量质子辐照引入了更多的辐照缺陷。

由图 5 可知,QW LD 的 V - I 特性对材料的位移效应比较敏感,而 V - I 特性也可以反映质子辐照后 QW LD 量子效率的改变。LD 的正向电流由扩散电流和空间电荷区的复合电流两部分组成,即

$$I = \frac{qn_i W A}{2\tau} \exp\left(\frac{qV}{2KT}\right) + \left(\frac{qAD_n^{1/2} n_{p0}}{\tau_n^{1/2}} + \frac{qAD_p^{1/2} p_{n0}}{\tau_p^{1/2}}\right) \exp\left(\frac{qV}{2KT}\right), \quad (5)$$

式中: W 为空间电荷区宽度; A 为器件有源区面积; n_i 为本征流子浓度; τ 为空间电荷区载流子寿命; τ_n 为 P 区的少子电子的寿命; τ_p 为 N 区的少子空穴的寿命; n_{p0} 为耗尽区 P 区一侧边缘处的平衡电子浓度; p_{n0} 为耗尽区 N 区一侧边缘处的平衡空穴浓度; D_n 和 D_p 分别为电子和空穴的扩散系数; V 为电压; K 为玻尔兹曼常数; T 为绝对温度。式(5)等号右侧的第一项为空间电荷区的复合电流,第二项为扩散电流。由图 5 可知器件偏

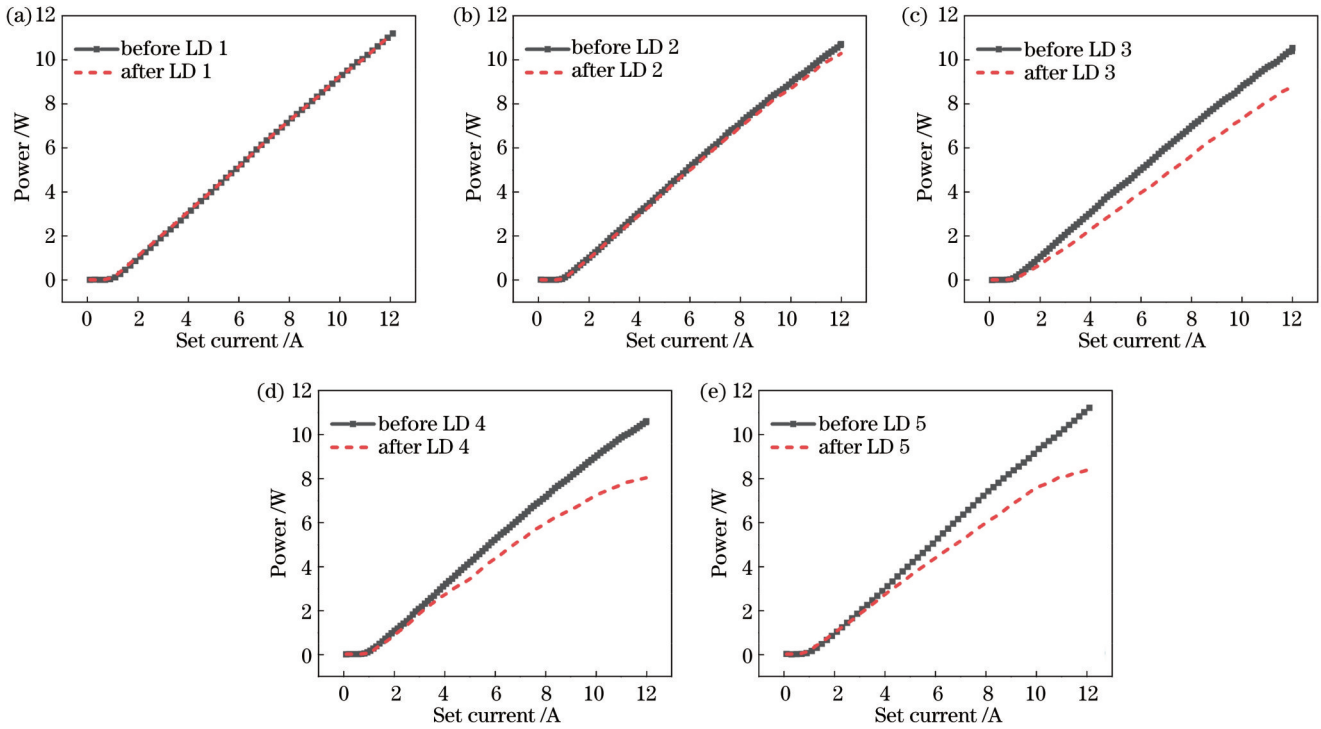


图 4 10 MeV 质子射入激光器前后的 P_{out} - I 特性。(a) $3 \times 10^8 \text{ cm}^{-2}$; (b) $3 \times 10^9 \text{ cm}^{-2}$; (c) $3 \times 10^{10} \text{ cm}^{-2}$; (d) $1 \times 10^{11} \text{ cm}^{-2}$; (e) $3 \times 10^{11} \text{ cm}^{-2}$

Fig. 4 P_{out} - I characteristics of LDs before and after 10 MeV proton injected. (a) $3 \times 10^8 \text{ cm}^{-2}$; (b) $3 \times 10^9 \text{ cm}^{-2}$; (c) $3 \times 10^{10} \text{ cm}^{-2}$; (d) $1 \times 10^{11} \text{ cm}^{-2}$; (e) $3 \times 10^{11} \text{ cm}^{-2}$

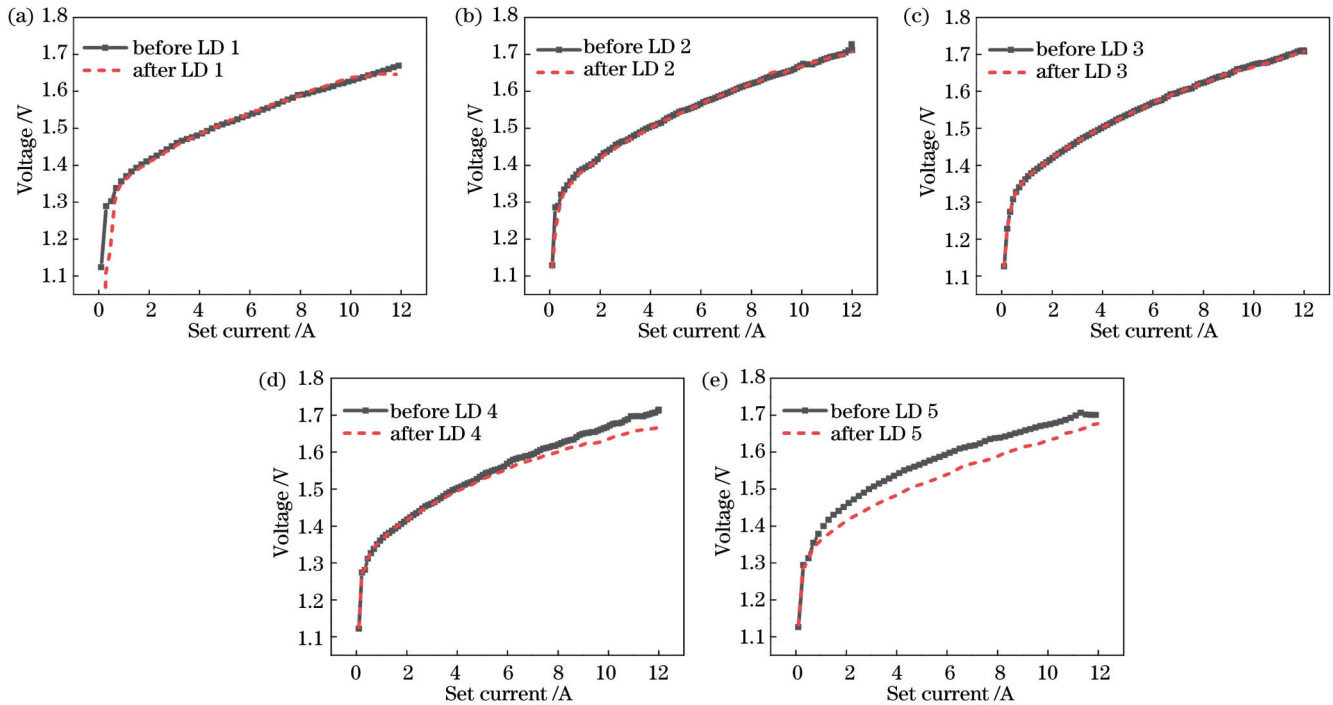


图 5 10 MeV 质子射入激光器前后的 V - I 特性。(a) $3 \times 10^8 \text{ cm}^{-2}$; (b) $3 \times 10^9 \text{ cm}^{-2}$; (c) $3 \times 10^{10} \text{ cm}^{-2}$; (d) $1 \times 10^{11} \text{ cm}^{-2}$; (e) $3 \times 10^{11} \text{ cm}^{-2}$

Fig. 5 V - I characteristics of LDs before and after 10 MeV proton injected. (a) $3 \times 10^8 \text{ cm}^{-2}$; (b) $3 \times 10^9 \text{ cm}^{-2}$; (c) $3 \times 10^{10} \text{ cm}^{-2}$; (d) $1 \times 10^{11} \text{ cm}^{-2}$; (e) $3 \times 10^{11} \text{ cm}^{-2}$

压特性下降,说明少子寿命下降,证明器件内部出现了少子陷阱,且少子陷阱浓度与辐照质子注量成正比。

继续将 P_{out} - I 数据代入式(2)得到质子辐照后器件的外微分量子效率,如图 7 所示,其中 $\Delta\eta_0$ 为辐照前与辐照

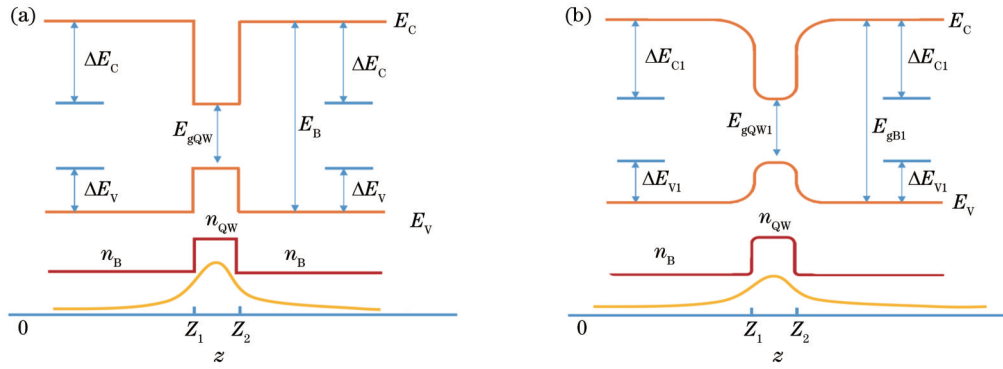


图 6 LD QW 处的带隙结构。(a)辐照前;(b)辐照后

Fig. 6 Band gap structure at QW of LD. (a) Unirradiated; (b) irradiated

后外微量子效率的差值。可以发现,所有 QW LD 的外微量子效率均下降,且下降程度与质子注量正相关但非线性相关,具体的相关性与作用机理还需要进一步研究。

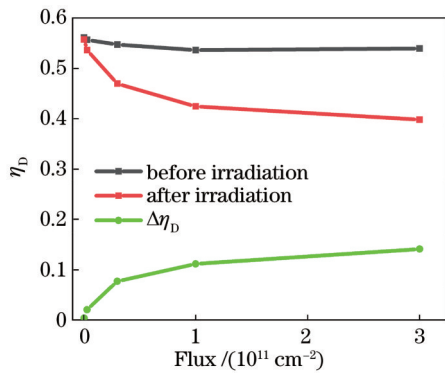


图 7 外微量子效率改变量与质子注量的关系

Fig. 7 Relation between change of external differential quantum efficiency and proton fluence

4 结 论

975 nm GaAs 基高功率 QW LD 的光电限制作用来源于 QW 与两侧材料的禁带宽度差和折射率差,故载流子迁移率、载流子寿命与异质结结构、杂质和缺陷散射有极大关联。质子辐照会通过弹性散射或非弹性散射使晶格原子脱离格点形成空位缺陷,并在外延层界面处形成缺陷密度峰值,而界面缺陷的增加会导致载流子受到散射的概率增加并影响载流子迁移率。同时,缺陷对载流子的俘获作用会使异质结处载流子积聚,导致能带弯曲受阻,载流子浓度降低。通过质子辐照模拟和实验证实,质子辐照会在器件内诱生多种空位缺陷,产生于有源区的缺陷会导致器件非辐射复合增加、外微量子效率下降,最终表现为器件的中心波长红移、光谱中杂峰增加和输出光功率显著下降,使器件的电光转化效率和可靠性整体下降。结合理论计算,明确了辐照注量与退化之间存在的正反馈数学关系。今后将继续深入研究偏压、温度等多物理场条件

下的 QW LD 位移损伤效应机理,为 GaAs 基 QW LD 和同类器件辐射应用前的可靠评估提供了进一步指导。

参 考 文 献

- [1] 乔闯, 苏瑞琪, 李翔, 等. 980 nm 高功率 DBR 半导体激光器的设计及工艺[J]. 中国激光, 2019, 46(7): 0701002. Qiao C, Su R G, Li X, et al. Design and fabrication of 980 nm distributed Bragg reflection semiconductor laser with high power [J]. Chinese Journal of Lasers, 2019, 46(7): 0701002.
- [2] 宋镇江, 张云昌, 黄秀军, 等. 975 nm 光纤耦合半导体激光器传能技术[J]. 空间电子技术, 2018, 15(2): 101-105. Song Z J, Zhang Y C, Huang X J, et al. Laser energy transmission technology based on 975 nm fiber coupling diode laser [J]. Space Electronic Technology, 2018, 15(2): 101-105.
- [3] 李俊伟, 石成英, 王祖军, 等. 不同能量质子辐照诱发子电池 GaAs 退化模拟研究[J]. 光学学报, 2021, 41(5): 0516003. Li J W, Shi C Y, Wang Z J, et al. Theoretical simulation on degradation of GaAs sub-cells induced by proton irradiation with different energies [J]. Acta Optica Sinica, 2021, 41(5): 0516003.
- [4] Robinson Z D, Adams J H Jr, Fisher J H, et al. Mission specific solar radiation environment model (MSSREM): peak flux model [J]. Space Weather, 2020, 18(8): 1-17.
- [5] 陈加伟, 李豫东, 玛丽娅, 等. 850 nm 垂直腔面发射激光器的辐射效应[J]. 红外与激光工程, 2022, 51(5): 20210326. Chen J W, Li Y D, Ma L Y, et al. Radiation effect of 850 nm vertical-cavity surface-emitting laser [J]. Infrared and Laser Engineering, 2022, 51(5): 20210326.
- [6] 王祖军, 宁浩, 薛院院, 等. 半导体激光器辐照损伤效应实验研究进展[J]. 半导体光电, 2020, 41(2): 151-158. Wang Z J, Ning H, Xue Y Y, et al. Research progresses of radiation damage experiments in laser diodes [J]. Semiconductor Optoelectronics, 2020, 41(2): 151-158.
- [7] Compton D M J, Cesena R A. Mechanisms of radiation effects on lasers [J]. IEEE Transactions on Nuclear Science, 1967, 14(6): 55-61.
- [8] Evans B D, Hager H E, Hughlock B W. 5.5-MeV proton irradiation of a strained quantum-well laser diode and a multiple quantum-well broadband LED [J]. IEEE Transactions on Nuclear Science, 1993, 40(6): 1645-1654.
- [9] Boutillier M, Gauthier-Lafaye O, Bonnefont S, et al. Measurement of irradiation impact on carrier lifetime in a quantum well laser diode [J]. IEEE Transactions on Nuclear Science, 2009, 56(4): 2155-2159.
- [10] 周义建, 陈校平, 曲光, 等. 基于马尔科夫过程的半导体激光器空间辐射可靠性分析[J]. 半导体光电, 2015, 36(1): 24-27, 33. Zhou Y J, Chen X P, Qu G, et al. Study on reliability of space

- irradiation of laser diodes based on Markov process[J]. *Semiconductor Optoelectronics*, 2015, 36(1): 24-27, 33.
- [11] 玛丽娅, 李豫东, 郭旗, 等. $\text{In}_{0.53}\text{Ga}_{0.47}\text{As}/\text{InP}$ 量子阱与体材料的 1 MeV 电子束辐照光致发光光谱研究[J]. *物理学报*, 2015, 64(15): 154217.
Ma L Y, Li Y D, Guo Q, et al. Photoluminescence spectra of 1 MeV electron beam irradiated $\text{In}_{0.53}\text{Ga}_{0.47}\text{As}/\text{InP}$ quantum well and bulk materials[J]. *Acta Physica Sinica*, 2015, 64(15): 154217.
- [12] 陈加伟, 李豫东, 玛丽娅·黑尼, 等. 850 nm 垂直腔面发射激光器的辐射效应和仿真[J]. *核技术*, 2022, 45(11): 110202.
Chen J W, Li Y D, Maria H, et al. Radiation effect and simulation of 850 nm vertical-cavity surface-emitting laser[J]. *Nuclear Techniques*, 2022, 45(11): 110202.
- [13] 宁浩. 辐照诱发半导体激光器性能退化实验研究与仿真模拟[D]. 湘潭: 湘潭大学, 2020: 26-50.
Ning H. Experimental research and analogue simulation of the performance degradation of laser diode induced by radiation[D]. Xiangtan: Xiangtan University, 2020: 26-50.
- [14] 李永宏, 寇勃晨, 赵耀林, 等. 质子在砷化镓材料中产生位移损伤的 Geant4 模拟[J]. *原子能科学技术*, 2018, 52(10): 1735-1739.
Li Y H, Kou B C, Zhao Y L, et al. Geant4 simulation of proton displacement damage in GaAs[J]. *Atomic Energy Science and Technology*, 2018, 52(10): 1735-1739.
- [15] 周书星, 方仁凤, 魏彦锋, 等. 磷化铟高电子迁移率晶体管外延结构材料抗电子辐照加固设计[J]. *物理学报*, 2022, 71(3): 037202.
Zhou S X, Fang R F, Wei Y F, et al. Structure parameters design of InP based high electron mobility transistor epitaxial materials to improve radiation-resistance ability[J]. *Acta Physica Sinica*, 2022, 71(3): 037202.
- [16] Srour J R, Palko J W. Displacement damage effects in irradiated semiconductor devices[J]. *IEEE Transactions on Nuclear Science*, 2013, 60(3): 1740-1766.
- [17] 张娜玲, 井红旗, 袁庆贺, 等. 不同 Al 组分的扩散阻挡层对无杂质空位诱导量子阱混杂的影响[J]. *中国激光*, 2021, 48(24): 2403001.
Zhang N L, Jing H Q, Yuan Q H, et al. Influence of diffusion barriers with different Al compositions on impurity-free vacancy induced quantum well mixing[J]. *Chinese Journal of Lasers*, 2021, 48(24): 2403001.
- [18] 王予晓, 朱凌妮, 仲莉, 等. Si_3N_4 沉积参数对量子阱混杂效果的影响[J]. *光学学报*, 2022, 42(10): 1031003.
Wang Y X, Zhu L N, Zhong L, et al. Influence of Si_3N_4 deposition parameters on intermixing of quantum wells[J]. *Acta Optica Sinica*, 2022, 42(10): 1031003.
- [19] Johnston A H. Radiation effects in optoelectronic devices[J]. *IEEE Transactions on Nuclear Science*, 2013, 60(3): 2054-2073.

Proton Displacement Damage in 975 nm Quantum Well Laser Diodes

Liu Cuicui¹, Jing Hongqi², Lin Nan^{2,3}, Guo Gang^{1*}, Ma Xiaoyu^{2,3**}

¹National Innovation Center of Radiation Application, China Institute of Atomic Energy, Beijing 102413, China;

²National Engineering Center for Optoelectronic Devices, Institute of Semiconductors, Chinese Academy of Sciences, Beijing 100083, China;

³College of Materials Science and Opto-Electronic Technology, University of Chinese Academy of Sciences, Beijing 100049, China

Abstract

Objective The development of deep space exploration and interstellar flight technology imposes higher requirements on the performance of spacecraft, especially on the energy power system and wireless communication system. However, in the typical satellite orbit region in space, the environment is filled with huge numbers of high-energy particles, such as protons, electrons, and heavy ions, due to the strong impact of solar proton events, Van Allen radiation belts, and galactic cosmic rays. Consequently, spacecraft are always exposed to the threat of various radiation effects caused by high-energy radiation particles, resulting in storage errors, communication losses, attitude losses, and other problems. In serious cases, the flight mission may fail instantaneously. The high-power near-infrared laser produced by the high-power 975 nm GaAs-based quantum well (QW) laser diode (LD) has outstanding advantages, such as high directivity, great monochromaticity, high optical power density, and long transmission distance. For this reason, such QW LDs have become the optimal choice to achieve long-distance wireless energy transmission and wireless communication in the complex space environment. Nevertheless, their development is seriously hindered by the harsh space environment and radiation effects. Therefore, to address the urgent need for major strategies in the radiation field, this paper studies the degradation law and triggering mechanism of high-power semiconductor QW LDs in radiation environments.

Methods The accelerator is investigated by ground simulated irradiation experiment and simulation calculation and analysis. Specifically, regarding the current typical spacecraft orbit, the accumulated 10 MeV proton equivalent displacement damage dose (DDD) is calculated under the condition that the spacecraft has been in orbit for 10 years, and its value is between $3 \times 10^8 \text{ cm}^{-2}$ and $3 \times 10^{11} \text{ cm}^{-2}$. Then, the 10 MeV proton irradiation experiment in vacuum at room temperature is carried out using the Beijing HI-13 tandem accelerator, and the optical power, volt-ampere characteristics,

and spectral performance of the LDs are tested before and after irradiation. Furthermore, Monte Carlo software simulation and theoretical calculation are performed to obtain the band structure and external differential quantum efficiency of the LDs before and after irradiation. The influence mechanism of material defects induced by proton irradiation and the changes in the interface and structure on the macroscopic performance of the LDs is analyzed in depth.

Results and Discussions The restrictions on the photons and electrons in the high-power 975 nm GaAs-based QW LD come from the band-gap difference and the refractive index difference of the materials among the QW and the junction barriers on both sides. Monte Carlo software simulation reveals that protons can induce vacancy defects by detaching the lattice atoms in the component materials of the LD from the lattice points through elastic scattering or inelastic scattering. In this case, a peak defect density can also be observed at the interface of each epitaxial layer near the active region. The results of the irradiation experiments show that 10 MeV proton irradiation at a fluence higher than $3 \times 10^{10} \text{ cm}^{-2}$ has a great influence on the electrical and optical properties of the LD. In contrast, the effect of 10 MeV proton irradiation at a fluence below $3 \times 10^8 \text{ cm}^{-2}$ on the electrical and optical properties of the LD is negligible. In addition, the degradation of the electrical and optical properties of the LD gradually aggravates as the accumulated proton fluence increases. As a result, macroscopic performance degradation phenomena can be observed, such as center wavelength shift, output power decline, threshold current increase, and volt-ampere characteristic deterioration. This indicates that more proton irradiation causes more severe performance degradation of the LD, ultimately resulting in more serious problems in stability and reliability.

Conclusions This study presents self-developed high-power 975 nm GaAs-based QW LDs and 10 MeV accelerator proton equivalent displacement damage irradiation experiments. The relationship between the performance degradation of the LD caused by the radiation effects and the accumulated proton fluence is analyzed by experimental tests and theoretical simulation methods, and the deep physical mechanism of the LD degradation induced by the radiation effects is clarified. The results suggest that the degree of the performance degradation of the LD as a result of the displacement damage effect is basically positively correlated with the accumulated fluence of proton irradiation, which causes severe performance degradation of the LD after a certain threshold is exceeded. Moreover, high-fluence proton irradiation produces more interface defects, which further increase the probability of carrier scattering, affect carrier mobility, and ultimately reduce the ability of the QW structure to restrict the photons and electrons. The defects in the active region turn into non-radiative recombination centers. They lead to the increased non-radiative recombination inside the LD and decreased external differential quantum efficiency and ultimately cause the macroscopic performance degradation of the irradiated LDs, such as the center wavelength shift, decreased output power, increased threshold current, and deteriorated volt-ampere characteristics. This research is expected to provide a useful reference for the reliable selection, performance evaluation, and radiation hardening of the 975 nm GaAs-based QW LD and other similar optoelectronic devices before their application in radiation environments, as well as for the improved performance of the radiation hardening design.

Key words quantum optics; quantum well laser diode; proton; displacement damage effect; performance evaluation